

Date Palm Pollen as a Promising Drug Delivery System: Release Kinetic Model and Antimicrobial Activity

Mahdi Shahriarinoor¹, Faten Divsar^{2,*}, Leila Youseftabar-Miri³,
Mohammad Banimahd Keivani²

1. Department of Microbiology, Rasht Branch, Islamic Azad University, Rasht, Iran

2. Department of Chemistry, Payame Noor University, P.O. BOX 19395-3697, Tehran, Iran

3. Department of Organic Chemistry, Faculty of Pharmaceutical Chemistry, Tehran Medical Sciences, Islamic Azad University, Tehran, Iran

Received: 14 August 2021

Accepted: 20 September 2021

DOI: 10.30473/ijac.2022.62531.1218

Abstract

Herein, the date palm pollen (DPP) grain was used as an amikacin (AMK) delivery vehicle for the first time. The AMK-loaded DPP was characterized using scanning electron microscopy (SEM), Fourier-transform infrared (FT-IR) spectroscopy, and surface area (BET) analysis. The pore size of DPP was obtained 80–200 nm that was favorable to the drug uptake. The effects of pH and temperature were studied on the AMK loading in DPP. The study of drug release kinetics in phosphate buffer pH 7.4 at 37 °C suggested that the best kinetic model was the Higuchi equation. The antibacterial activity of AMK-loaded DPP (AMK-DPP) was investigated on *Staphylococcus aureus* and *Escherichia coli* bacteria by the agar-well diffusion method. Minimum inhibitory concentration (MIC) and minimum bactericidal concentration (MBC) for AMK were also carried out by using broth dilution method. The similarity of the results between MIC and MBC is considerable. However, an intense reduction in the MBC was observed after AMK loaded on palm pollen. Moreover, the AMK-DPP was utilized to improve the effectiveness of AMK against the dangerous forms of antibiotic-resistant bacteria. In general, AMK-DPP shows to be a new favorable method allowing in the management of Gram-positive and Gram-negative bacterial infections and may be further evaluated in in-vivo experiments.

Keywords

Keywords: Palm Pollen; Bacterial Infections; Kinetic Studies.

1. INTRODUCTION

Staphylococcus aureus (*S. aureus*) and *Escherichia coli* (*E. coli*) are capable to cause a wide range of infections [1-3]. These bacteria can become pathogenic following a perturbation to their host (e.g., disease, wound, medication, prior infection, immunodeficiency, and aging). They have a critical role in opportunistic infection because of their multiple virulence factors that include protein A, coagulase, collagenase, hyaluronidase, hemolysins, lipases, different toxins, adhesive proteins, and also proteins affecting the biofilm formation. Various mechanisms caused *S. aureus* and *E. coli* bacteria to display resistance to many different antibiotics. Antibiotic resistance is a growing public health concern and has become increasingly widespread in the world [4-6]. Due to their rising rate, there is urgent to detect novel antimicrobial compounds [7].

In the past few decades, some antibiotics have been introduced with more efficiency, but none of them have improved activity against multi-resistant bacteria after a short period of time. In addition, in some cases the use of antibiotics alone does not produce the ideal operative inhibitory effects;

accordingly a combination of drugs with plant extract often imposes their synergistic effect which surpasses their individual performance [8].

Plant-derived materials are novel and robust vehicles for drug delivery which improve the stability and bioavailability of the active ingredient, also enhance the drug performance [9]. Pollen, the male reproductive element of flowers, can stimulate special attention in the biomedical research field due to its significant advantages in many aspects such as biocompatibility, tuneable pore size, and large specific surface area in addition to medicinal properties [10, 11]. Plants pollen as a natural porous carrier provides a synergism effect to inhibit a particular species of microorganisms. Pollen grains could be used to protect and deliver a range of different drugs and facilitate the release of antibiotics on a specific target. The pollen shells also develop new techniques to tackle antibiotic resistance and can effectively protect the light-sensitive antibiotics from rapid decomposition [12].

The antimicrobial activity of natural pollen has already been confirmed against human bacterial pathogens, human fungal pathogens, and different plant pathogens [13, 14]. Moreover, they could be

*Corresponding Author: f.divsar@pnu.ac.ir

an important tool in fighting against antimicrobial resistance. Metwaly et al. demonstrated that palm pollen extract showed both anti-inflammatory and anti-apoptotic activities and it can be used to develop new herbal medicine [15]. The natural bee-bread and bee-pollen from different aromatic and medicinal plants were studied for their antimicrobial activities on antibiotic-resistant bacterial strains isolated from human pathology. All samples showed strong antimicrobial activities on the bacterial strains, first tested for their resistance to antibiotics [16].

Given these particular features, the microcapsules extracted from the pollens of *Corylus avellana* were employed as a carrier for pantoprazole delivery [17]. There are only a few reports concerning the use of DPP as a vehicle for drugs [18]. Alshehri et al. extracted sporopollenin capsules from date palm (*Phoenix dactylifera* L.) spores and coated them by natural polymer composite (chitosan with glutaraldehyde). The polymer-coated macroporous capsules were used in the in vitro-controlled delivery of ibuprofen and paracetamol [19, 20]. AMK demonstrated an improved efficiency in long-term clinical treatment, due to its chemical structure that has fewer points susceptible to enzymatic inactivation than the other aminoglycosides [21]. Herein, the model of in vitro release of antibiotics from the AMK-DPP was studied for the first time. Afterward, the antimicrobial efficiency of AMK laden porous scaffold DPP was studied and measured with the free (untrapped) drug as a control against *S. aureus* and *E. coli* bacteria.

2. EXPERIMENTAL

2.1. Chemicals and apparatus

DPP (*Phoenix dactylifera* L.) was obtained from trees grown at an agricultural research station orchard of Azizabad, Bam, Kerman, Iran. AMK antibiotics were purchased from Merck Company (Merck, Germany). The strains, including *S. aureus* PTCC 1431 and *E. coli* PTCC 1396 were prepared from the archive section of the microbiology department, Rasht branch of Islamic Azad University.

FT-IR spectra of untreated DPP, AMK, and AMK-DPP were analyzed by using a Perkin Elmer 100 FT-IR Spectrometer in the 400–4000 cm^{-1} region. The morphology and size of the sample were determined by using a field emission scanning electron microscopy (FESEM) analysis. The nitrogen adsorption-desorption analysis was performed using a BETSORP-mini II (Microtrac BEL, Japan) to examine the Brunauer-Emmett-Teller (BET) surface area and pore size distribution. AMK concentration in the solution was quantitatively determined by measuring the

absorbance at a maximum wavelength of 565 nm using a UV-Vis spectrophotometer (Unico, Model SQ2800, USA).

2.2. Loading AMK into the DPP

20 mg of DPP was added to 50 mL of distilled water at room temperature under magnetic stirring. As well, 25 mg AMK was dissolved in 5 mL of distilled water by gently stirring at 25°C and then was added to DPP suspension and stirred at room temperature for certain time. AMK–DPP suspension was centrifuged at 4000 rpm for about 15 min and the supernatant was separated. With regard to determination of the AMK amount loaded into the DPP, the absorbance of the suspension was determined at wavelength of 565 nm and assigning it to the standard calibration curve. The next equations given below were utilized to calculate the amount of loaded drug and the percentage loading (%) of AMK:

$$\text{Amount of drug (mg)} = (\text{Absorbance} \times \text{dilution factor}) / (\text{Slope} \times 1000) \quad (1)$$

$$\text{Loading content (\%)} = (\text{Amount of drug into DPP} / \text{Initial amount of DPP}) \times 100 \quad (2)$$

$$\text{Drug loading efficiency (\%)} = (\text{Amount of loaded drug} / \text{Amount of drug in feed}) \times 100 \quad (3)$$

The effect of different parameters such as loading time, pH and temperature of the solution were investigated for drug loading efficiency into AMK-DPP. The control of solution pH was performed by a pH meter and adding 0.1 M hydrochloric acid and sodium hydroxide.

2.3. In vitro drug release study

The AMK delivery rate was determined by solving 10 mg of dry powder of AMK-DPP into 10 ml of phosphate buffered saline (PBS) in pH=7.4, then was preserved at 37 °C with continuous magnetic stirring. At different time intervals, 2 mL of release media was gathered and centrifuged to identify the amount of AMK. The withdrawn solution was replaced with an equal volume of fresh buffer to keep the total volume constant. The drug amount of the cumulative release from the AMK-DPP was calculated with a standard calibration curve.

$$\text{Amount of AMK (mg/mL)} = (\text{Absorbance} / \text{Slope}) \pm \text{intercept} \quad (4)$$

$$\text{Milligram of AMK} = (\text{Concentration} \times \text{Volume of dissolvent buffer}) \quad (5)$$

$$\text{Collective release (\%)} = [\text{Volume of sample withdrawn (ml)} / \text{Bath volume (ml)}] \times P_{(t-1)} + P_t \quad (6)$$

where P_t is the percentage release at time t and $P_{(t-1)}$ is the percentage release previous to t .

Several mathematical equations have been established to determine the kinetic model of the release of the loaded drug [22]. The drug release kinetics were most often analyzed using kinetic models such as zero- and first-order, and Higuchi.

In this study, the three models were evaluated to recognize the *in vitro* delivery kinetics of AMK from the porous pollen carrier. In a zero-order reaction, the rate is supposedly liberated of the reactant amount. The zero-order kinetics model is as the following equation:

$$Q_t = Q_0 + k_0 t \quad (7)$$

where t is the time and Q_0 and Q_t are the amounts of released drug in the initial time and in the t time, respectively. k_0 is the constant of zero-order rate. To determine the release mechanism, the value of K_0 was obtained from the slope of the linear plot of cumulative amount of drug release against the time. The model of the first-order kinetics can be measured by the equation [23];

$$\log Q_t = \log Q_0 + k_1 t / 2.303 \quad (8)$$

where Q_t is the collective drug concentration released in the period of t time, Q_0 is the primary concentration of the drug in the solution, k_1 is the constant of the first-order model and t presents the time. The logarithm of collective amount of the released AMK was recorded against time and $k_1/2.303$ is calculated through the slope of the achieved line.

Higuchi model which is based on the Fickian diffusion control is calculated by the simplified Higuchi equation [24];

$$Q_t = Q_0 + k_H t^{1/2} \quad (9)$$

where k_H is the Higuchi constant in the time t . Concerning to obtain the kinetics of the drug release, the plot of collective amount of liberated drug versus the square root of time was prepared. Thermodynamic factors like the change in the Gibbs free energy (ΔG° , kJ/mol), enthalpy (ΔH° , kJ/mol) and entropy (ΔS° , J/mol.K) can be used as indicators for practical applications. The thermodynamic results were obtained at 298, 308, 318 and 328 K. To determine these parameters of AMK release, the K_d values were calculated using the Van't Hoff equation:

$$\Delta G = -RT \ln K_d \quad (10)$$

$$K_d = \frac{q_e}{C_e} \quad (11)$$

$$\Delta G = \Delta H - T \Delta S \quad (12)$$

(K_d = the distribution coefficient, T = temperature (K), R = the gas constant (8.3145 J/mol.K), C_e = equilibrium concentration of AMK in water (mg/L), q_e = the amount of the release AMK per unit mass of the adsorbent (mg/g)).

2.4. Antibacterial activity of DPP, AMK, and AMK-DPP

The antibacterial activity of DPP was tested against *S. aureus* and *E. coli* strains by the agar-well diffusion method. *S. aureus* and *E. coli* (0.5 McFarland turbidity) were prepared in Mueller-Hinton broth and were plated onto Mueller-Hinton agar directions by sterile swabs. Afterward, wells were punched in the plates using a sterile stainless steel borer. The wells were filled with 0.25, 0.5, 1,

and 2 mg/ml palm pollen water extract per well. The plates were incubated at 37 °C for 24 h. The diameters of the inhibition zones were measured in millimeters.

In addition, the antibacterial activity of AMK and AMK-DPP was conducted against *S. aureus* and *E. coli* strains using the agar-well diffusion method. Afterward, minimum inhibitory concentration (MIC) and minimum bactericidal concentration (MBC) for AMK and AMK-DPP were carried out by using broth dilution method according to clinical and laboratory standard institute guideline (CLSI). Therefore, the different concentrations of AMK and also AMK-DPP in the range of 0.19-100 (mg/ml) were tested. Next to 24 and 48 h incubation at 35°C–37°C, the test tubes were determined for probable bacterial turbidity, MBC and MIC of each test compound was examined individually.

3. RESULT AND DISCUSSION

3.1. Characterization of AMK-DPP

Fig. 1 depicts the preparation process of AMK-DPP and also its antimicrobial activity in comparison to the AMK and the bare DPP against *S. aureus* and *E. coli*.

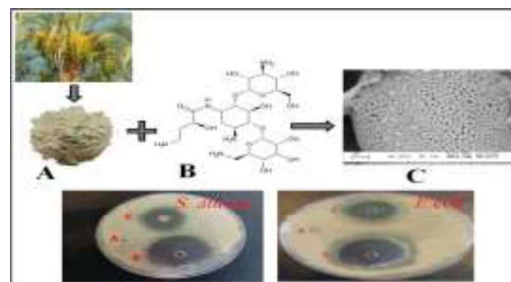


Fig. 1. Schematic diagram of the AMK-DPP preparation and its antimicrobial activity, (A) DPP, (B) AMK, and (C) AMK-DPP.

The presence of different functional groups on the surface of the raw DPP, AMK antibiotic and AMK-DPP were identified by FTIR analysis (Fig. 2). The comparison of the spectra represents the successful interaction between AMK and DPP scaffold. The presence of hydroxyl groups of alcoholic and phenolic fragments in pectin, cellulose and lignin structures produce the broad peak at 3406.05 cm^{-1} in the spectrum of the palm pollen (Fig. 2A), the is due to. The peaks detected at 2923.83 and 2854.45 cm^{-1} can be attributed to the stretching vibrations of the aliphatic C-H. The peak observed at 1658.67 is due to C=C groups and 1546.50 cm^{-1} can be assigned to carbonyl groups of the protein amide I linkage in the pollen structure. In addition, the peaks at 1456.16 and 1409.78 cm^{-1} are related to the C-N stretching and N-H bending of the protein amide II linkage. The C-OH stretching vibration and the C-

O–C stretching of cellulose appeared at 1051.13 and 999.06 cm^{-1} , respectively.

FT-IR spectrum of the AMK is shown in Fig. 2B. The broad peak appeared at 3384.84 and 3255.62 cm^{-1} is due to the strong hydrogen bonding of phenolic –OH groups. The characteristic absorption band of substituted amide groups and the aromatic C–H stretching vibration are observed at 3049.25 and 2916.17 cm^{-1} , respectively. The sharp peak at 1639.38 cm^{-1} is due to the C=O stretching of amide groups. Double aromatic C=C stretching vibrations which related to phenyl ring observed at 1535.23 cm^{-1} and 1448.44 cm^{-1} , since the interaction between aromatic ring and ring substituent. C–N stretching vibration appeared at 1108.99 cm^{-1} .

After loading AMK into the DPP, characteristic variations were monitored in the AMK spectrum as revealed in Fig. 2C. Where some peaks in the spectrum were changed or missed and new peaks appeared. The absorption band in 3417.63 cm^{-1} represents the free hydroxyl groups on the surface of AMK. The C=O stretching band (1739.67 cm^{-1}) of unsaturated fatty acids at the pollen overlapped with the aromatic C–C stretching band (1679.88 cm^{-1}) of AMK and these peaks obscure the C=C peak of AMK at 1650.95 cm^{-1} . The peaks in 1554.52 and 1514.02 represent the absorption area of N–H of AMK. Peaks in the range of 1460.01 to 1425.30 demonstrate stretching vibration of C–O–H groups, while a peak at 1039.56 cm^{-1} was shown C–N band.

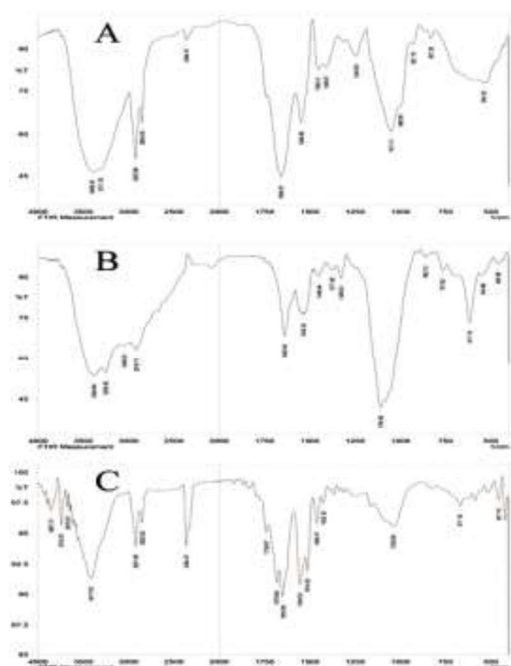


Fig. 2. FT-IR spectra of (A) DPP, (B) AMK, and (C) AMK-DPP grains.

The morphology and particle size of the DPP and AMK-DPP were studied using SEM image. As is seen from Fig. 3A, DPP has the highly porous and reticulate surface structure. The pores size of DPP is in the range 80-200 nm. Moreover, the chemical treatment in the extraction procedure increases the number and the scale of the holes on the superficial of pollen grain as a consequence. On the other hand, Fig. 3B, obviously approves that the AMK was successfully placed in the porous host.

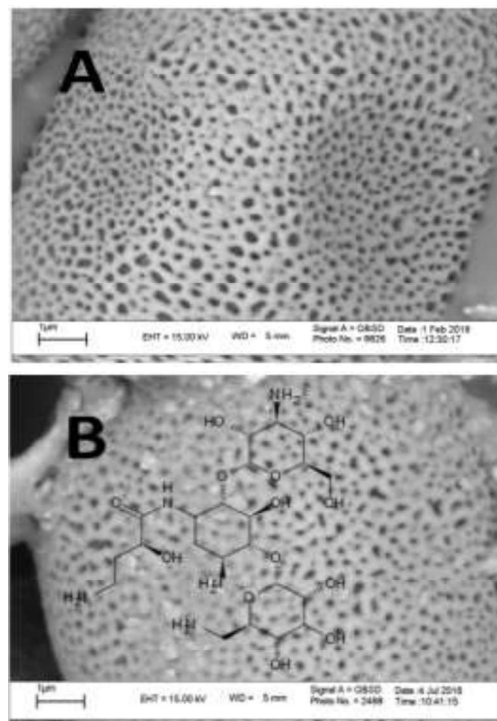


Fig. 3. SEM image of (A) DPP and (B) AMK-DPP.

3.2. Porosity and surface area measurement

BET analysis of DPP and AMK-DPP samples provide specific surface area evaluation based on nitrogen multilayer adsorption/desorption isotherms as a function of relative pressure (Fig. 4). Consistently both adsorption/desorption curves displayed the same type IV isotherms, with a characteristic hysteresis loop (H3) which can be associated with a porous structure [25]. The important structural information derived from the nitrogen adsorption-desorption isotherms and pore diameters of DPP and DPP- AMK are listed in Table 1.

Table 1. The elements of BET and BJH of DPP and DPP- AMK.

	S_{BET} (m^2g^{-1})	V_{BJH} (cm^3g^{-1})	D_{Pore} (nm)
DPP	15.00	0.059	9.07
AMK-DPP	8.51	0.031	6.42

BET surface area (S_{BET}) evaluated in the range of relative pressure (p/p_0) 0.0 to 0.99; V_{BJH} = pore volume at STP; D_{Pore} = mean pore diameter

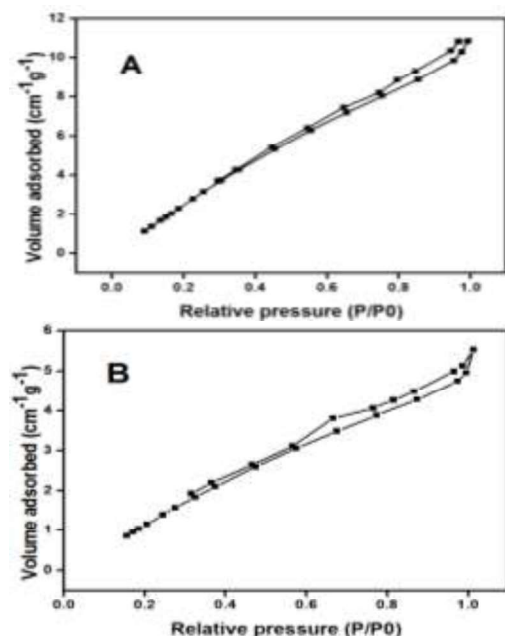


Fig. 4. Nitrogen adsorption-desorption isotherm (A) DPP and (B) AMK-DPP.

3.3. The drug loading conditions

The pH of aqueous solution of the AMK is an important factor that influences its uptake into the DPP. As shown in Fig. 5A, the range 2–10 of pH was investigated. The maximum increase in the loading of AMK on DPP was obtained in pH 7, and after that, the rate of loading was reduced. At physiological pH, the amino groups of AMK largely hold a positive charge [26], which may encourage the interaction of the amino groups of AMK with the surface of the DPP and, hence, increase the adsorption of AMK into the porous DPP. At lower pH values, drug loading was restricted probably due to the competition between H^+ and positively charged drug on the vacant adsorption sites. This leads to lowering of the adsorption capacity. Palm pollen grains are lignocellulosic materials, consisting of vital components such as polyphenolic compounds and flavonoids. However, no important difference was found in adsorption at pH 5.8 and 7.0, proposing that ionic interactions are not the only mechanism [27]. Temperature is the other important parameter on the drug entrapment efficiency; therefore, the loading of the AMK into DPP was analyzed at different temperatures (25–55 °C). It was shown that increasing of the temperature resulted to the increasing of the adsorption value, which proposed the endothermic nature of the sorption process (Fig. 5B). The loading AMK into DPP was

performed in the various contact time (1–5 h). Fig. 5C reveals that at a primary step, the sorption of AMK was rapid, and the equilibrium was achieved after 2 h.

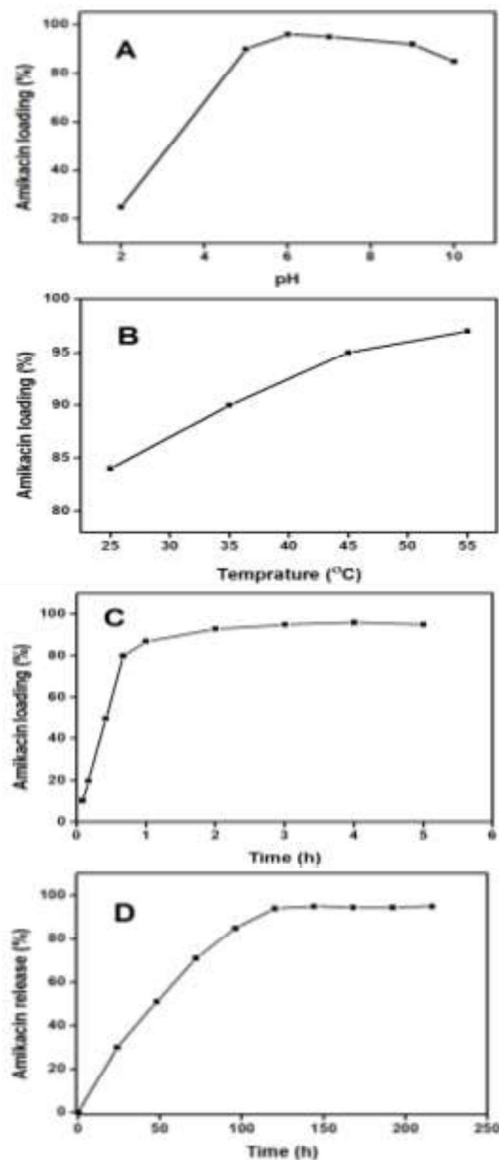


Fig. 5. The effect of (A) pH, (B) temperature, and (C) time on the drug loading efficiency, (D) Release profile of AMK from AMK-DPP in PBS solution at pH 7.4.

The *in vitro* gradual release profile of AMK from AMK-DPP was investigated in PBS (pH 7.4, 37 °C) during 220 hours of incubation (Fig. 5D). It can be seen that AMK releases from AMK-DPP with a primary “burst” release followed by a slower release due to the concentration gradient. The percentage of AMK release was increased with increasing time and after 120 hours release percentage remained almost stable. Nowadays, some researchers are examining plants or

nanoparticles as a delivery system for increasing antibiotic effect on some bacteria. The findings are consistent with the previous studies that revealed the pollen grains have an antibacterial effect and can be used effectively for drug delivery [28,29].

3.4. In vitro release kinetics

Fig. 6. shows the results of kinetic and thermodynamic studies for the release of AMK from AMK-DPP sorbent. Table 2 lists the kinetic elements of the release process obtained from the different release kinetics mechanisms.

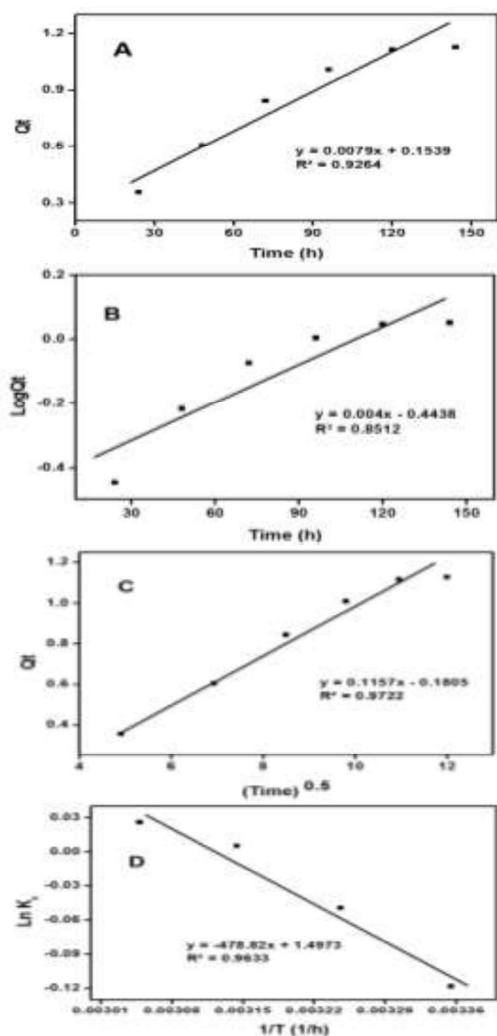


Fig. 6. Release rate curves of AMK from the AMK-DPP sorbent(A) zero order,(B) first order and (C) Higuchi model, and (D)thermodynamic data in the different temperatures 293, 308, 318, and 328 K in pH 7.4 and 10 mg of AMK-DPP.

The best correlation coefficient (R^2) was obtained in the Higuchi model. The release kinetic data in the Table 2 reveal that Higuchi equation is a more

suitable model for the AMK loaded AMK-DPP. It can be resulted that release kinetic model of AMK was due to Fickian diffusion. Accordingly, it can be recommended that release kinetics of AMK loaded AMK-DPP are organized by Fickian diffusion.

Table 2. Model compounds of the kinetic studies on AMK release from the AMK-DPP.

Kinetics models	zero-order		First -order		Higuchi	
	R^2	K_1	R^2	K_2	R^2	K_H
AMK-DPP	0.9264	0.0079	0.8512	0.004	0.9722	0.1157

Table 3. Values of thermodynamic parameters of release of AMK from the AMK-DPP.

ΔH° (J/mol)	ΔS° (J/mol)	ΔG° (kJ/mol)			
		298 K	308K	318K	328K
3981	12.45	292.85	126.5	-	-
				13.75	70.90

Actually, important parameters such as the change of enthalpy ΔH , the change of entropy ΔS and the change of the total free energy ΔG that occur during the binding processes are global properties of the systems. These parameters have been determined to a wide range of chemical and biochemical binding interactions [30]. The data in the Table 3 show negative ΔG° values achieved in higher temperatures that are reflected to the spontaneity of the process. The positive ΔS° values point to increased disorder at the DPP/solution interfaces through the release process. The antimicrobial activity of DPP, AMK and AMK-DPP was assessed by well-diffusion agar. Inhibition zone observed both of AMK and AMK-DPP have significant antimicrobial activity. As shown in Fig. 7 (a) and (b), the inhibition zone of AMK against *S. aureus* is 28 mm although it is 37 against *E. coli*, but in case of AMK-DPP, the inhibition zone against *S. aureus* is 35 mm and it is 45 mm against *E. coli*. The DPP alone showed no antimicrobial activity. The results of antibacterial activity revealed that DPP is a promising carrier for AMK. According to the inhibition zone, *E.coli* is more susceptible to AMK and AMK-DPP than *S. aureus*.

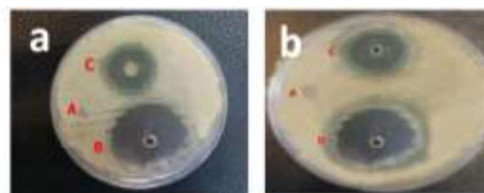


Fig. 7. Inhibition zone of; (A) DPP, (B) AMK, and (C) AMK-DPP against (a) *S. aureus* and (b) *E.coli*.

In this analysis, various concentrations of AMK and AMK-DPP displayed MIC and MBC against *S. aureus* and *E. coli*. The MIC and MBC tests are presented in Table 4 in detail. The results showed that there is a decrease in the MIC in the case of AMK-DPP in comparison to AMK. The most interesting point is the reduction in the MBC for AMK-DPP which implies that DPP increased the antibacterial activity and the effectiveness of AMK versus *S. aureus* and *E. coli*. Moreover, the obtained data revealed that there is a decrease in the MIC and MBC in case of AMK-DPP compared to AMK alone which implies DPP as a delivery system improved the effectiveness of AMK. Similar results about synergism effect of plant extract with antibiotics were reported [31].

Table 4. Result of MIC and MBC test against *S. aureus* and *E. coli*.

Bacteria	<i>E. coli</i>		<i>S. aureus</i>	
	AMK	AMK-DPP	AMK	AMK-DPP
MIC	25	12.5	25	6.5
MBC	50	25	50	12.5

MIC (mg/mL) = minimum inhibitory concentration that is lowest concentration to completely inhibit bacterial growth, MBC (mg/mL) = the lowest amount of bacterial that is minimum amount to totally kill the bacteria.

4. CONCLUSION

For the first time AMK was successfully incorporated in the porous scaffold of DPP as a drug delivery system for improving the effectiveness of AMK against *S. aureus* and *E. coli*. The AMK-DPP presented a smaller MIC and MBC than AMK and DPP separately. Therefore, it can assume that AMK might be managed in lesser doses or extended intervals by following DPP to decrease their side effects. The kinetics study on drug release indicated that the release mechanism could be described as Fickian diffusion model. In addition, the DPP as an intelligent pH-responsive carrier not only protected the AMK structure but also showed the controlled drug release in the acidic environment of the stomach to the alkaline intestinal that made hopes to provide oral formulation of the medicine. Moreover, the structure of the DPP did not change after the release of drug indicates the porous structure of DPP for drug loading and release was stable. Consequently, developing investigations on the AMK-DPP for animal models with antibiotic resistant infections are recommended.

ACKNOWLEDGEMENTS

We would like to thank our colleagues in Research Council of the University of Islamic Azad University, Rasht Branch and Tehran Medical

Sciences, and Payame Noor University for providing a good contribution to all aspects of the project.

Compliance with ethical standards

The study was carried out in accordance with ethical standards in all aspects.

Conflict of interest The authors declare no conflict of interest.

REFERENCES

- [1] S. Ganapathy, S. Karpagam, In vitro evaluation of antibacterial potential of *Andrographis paniculata* against resistant bacterial pathogens Methicillin Resistant *Staphylococcus aureus* (MRSA) and Multiple Drug Resistant *Escherichia coli* (MDR *E. coli*), *J. Pharmacogn. Phytochem.*, 5 (2016) 253.
- [2] K. Winkler, C. Simon, M. Finke, K. Bleses, M. Birke, N. Szentmáry, D. Hüttenberger, T. Eppig, T. Stachon, A. Langenbacher, HJ Foth, M. Herrmann, B. Seitz, M. Bischoff, Photodynamic inactivation of multidrug-resistant *Staphylococcus aureus* by chlorin e6 and red light ($\lambda = 670$ nm), *J Photochem Photobiol B.*, 162 (2016) 340-347.
- [3] P. Hassanzadeh, Y. Hassanzadeh, J. Mardaneh, E. Rezai, M. Motamedifar, Isolation of methicillin-resistant *Staphylococcus aureus* (MRSA) from HIV patients referring to HIV referral center, Shiraz, Iran, 2011-2012., *Iran. J. Med. Sci.*, 40 (2015)526-530.
- [4] M. Shahriarinoor, F. Divsar, Z. Eskandari, Synthesis, characterization, and antibacterial activity of thymol loaded SBA-15 mesoporous silica nanoparticles, *Nano-Met. Chem.* 49 (2019) 182-189.
- [5] B. Marasa, S. Iram, K. Sung, O. Kweon, C. Cerniglia, S. Khan, Molecular characterization of fluoroquinolone resistance of methicillin-resistant clinical *Staphylococcus aureus* isolates from Rawalpindi, Pakistan, *Med. Res. Arch.*, 2 (2015) 1-14.
- [6] K.L. Painter, E. Strange, J. Parkhill, K. B. Bamford, D. Armstrong-James, A. M. Edwards, *Staphylococcus aureus* Adapts to Oxidative Stress by Producing H₂O₂-Resistant Small-Colony Variants via the SOS Response, *Infect. Immun.*, 83 (2015) 1830-1844.
- [7] G. Adwan, B. Abu-Shanab, K. Adwan K, Antibacterial activities of some plant extracts alone and in combination with different antimicrobials against multidrug-resistant *Pseudomonas aeruginosa* strains, *J. Trop. Med.*, 3 (2010) 266-269.

- [8] S Chanda, K Rakholiya, *Microbiol. Book Series*, Combination therapy: Synergism between natural plant extracts and antibiotics against infectious diseases, 1(2011) 520-529.
- [9] R. Mohammadinejad, S. Karimi, S. Irvani, R.S. Varma, Plant-derived nanostructures: types and applications, *Green Chem.*, 18 (2016) 20-52.
- [10] S.A. Jassim, M.A. Najji, In vitro Evaluation of the Antiviral Activity of an Extract of Date Palm (*Phoenix dactylifera* L.) Pits on a Pseudomonas Phage, *Evid Based Complement Alternat Med.*, 7 (2010) 57-62.
- [11] F. Masmoudi-Allouche, S. Touati, K. Mnafigui, N. Gharsallah, A. El Feki, N. Allouche, Phytochemical profile, antioxidant, antibacterial, antidiabetic and anti-obesity activities of fruits and pits from date palm (*Phoenix dactylifera* L.) grown in south of Tunisia, *J Pharmacogn. Phytochem.*, 5 (2016) 15-22.
- [12] C.S. Bailey, J.S. Zarins-Tutt, M. Agbo, H. Gao, A. Diego-Taboada, M. Gan, R.B. Hamed, E.R. Abraham, G. Mackenzie, P.A. Evans, R.J.M. Goss, A natural solution to photoprotection and isolation of the potent polyene antibiotic, marinomycin A, *Chem. Sci.*, 10 (2019) 7549-7553
- [13] C.E. Beneke, A.M. Viljoen, J.H. Hamman, Polymeric Plant-derived Excipients in Drug Delivery, *Molecules*, 14 (2009) 2602-2620.
- [14] S.M. Moghimi, A.C. Hunter, J.C. Murray, Long-circulating and target-specific nanoparticles: theory to practice, *Pharmacol. Rev.*, 53 (2001) 283-318.
- [15] M.S. Metwaly, M.A. Dkhil, S. Al-Quraishy, Anti-coccidial and anti-apoptotic activities of palm pollen grains on *Eimeria papillata*-induced infection in mice, *Biol. Sect. zool.*, 69 (2014) 254-259.
- [16] Z. Abouda, I. Zerdani, I. Kalalou, M. Faïd and M.T. Ahami., The Antibacterial Activity of Moroccan Bee Bread and Bee-Pollen (Fresh and Dried) against Pathogenic Bacteria, *Res. J. Microbiol.*, 6 (2011) 376-384.
- [17] L. Akyuz, I. Sargin, M. Kaya, T. Ceter, I. Akata, A new pollen-derived microcarrier for pantoprazole delivery, *Mater. Sci. Eng. C*, 71 (2017) 937-942.
- [18] Saraf S, Applications of novel drug delivery system for herbal formulations, *Fitoterapia*, 81 (2010) 680-689.
- [19] S.M. Alshehri, H.A. Al-Lohedan, E. Al-Farraj, N. Alhokbany, A.A. Chaudhary, T. Ahamad, Macroporous natural capsules extracted from *Phoenix dactylifera* L. spore and their application in oral drugs delivery, *Int. J. Pharm.*, 504 (2016) 39-47.
- [20] S.M. Alshehri, H.A. Al-Lohedan, A.A. Chaudhary, E. Al-Farraj, N. Alhokbany, Z. Issa, S. Alhousine, T. Ahamad, Delivery of ibuprofen by natural macroporous sporopollenin exine capsules extracted from *Phoenix dactylifera* L., *Eur. J. Pharm. Sci.*, 88 (2016) 158-165.
- [21] S. Ghaffari, J. Varshosaz, A. Saadat, F. Atyabi, Stability and antimicrobial effect of amikacin-loaded solid lipid nanoparticles, *Int. J. Nanomedicine*, 6 (2011) 35-43.
- [22] L. Zhao, Y. Wei, Y. Mei, L. Yang, Y. You, X. Yang, Y. Jiang, Preparation and in Vitro Drug Release Evaluation of Once-Daily Metformin Hydrochloride Sustained-Release Tablets, *Pharmacol. Pharm.*, 3 (2012) 468-473.
- [23] P. Costa, J.M.S. Lobo, Modeling and comparison of dissolution profiles, *Eur. J. Pharm. Sci.*, 13 (2001) 123-133.
- [24] T. Higuchi, Mechanism of sustained-action medication. Theoretical analysis of rate of release of solid drugs dispersed in solid matrices, *J. Pharm. Sci.*, 52 (1963) 1145-1149.
- [25] Adelkhani H., Ghaemi M., Ruzbehani M., Evaluation of the Porosity and the Nanostructure Morphology of MnO₂ Prepared by Pulse Current Electrodeposition, *Int. J. Electrochem. Sci.*, 6 (2011) 123-135.
- [26] A. Forge, J. Schacht, Aminoglycoside antibiotics, *Audiol. Neurootol.*, 5 (2000) 3-22.
- [27] M. Shafiq, A.A. Alazba, M.T. Amin., Removal of heavy metals from wastewater using date palm as a biosorbent: a comparative review, *Sains Malays.*, 47 (2018) 35-49.
- [28] A. Diego-Taboada, ST. Beckett, S.L. Atkin, G. Mackenzie, Hollow Pollen Shells to Enhance Drug Delivery, *Pharmaceutics*, 6 (2014) 80-96.
- [29] A.K.F. Dyab, M.A. Mohamed, N.M. Meligi, S.K. Mohamed, Encapsulation of erythromycin and bacitracin antibiotics into natural sporopollenin microcapsules: antibacterial, cytotoxicity, in vitro and in vivo release studies for enhanced bioavailability, *RSC Adv.*, 8 (2018) 33432-33444.
- [30] A. Arnaud, L. Bouteiller, Isothermal titration calorimetry of supramolecular polymers, *Langmuir*, 20 (2004) 6858-6863.
- [31] S.A. Saquib, N.A. AlQahtani, I. Ahmad, M. Abdul Kader, S.S. Al Shahrani, E.A. Asiri, antibiotics Evaluation and Comparison of Antibacterial Efficacy of Herbal Extracts in Combination with Antibiotics on Periodontal pathogens: An in vitro Microbiological Study, *Antibiotics*, 8 (2019) 89-101.

گرده خرما به عنوان یک سیستم دارورسانی امیدوارکننده: بررسی سینتیک رهایش و فعالیت ضد میکروبی

مهدی شهریاری نور^۱، فاتن دیو سر*^۲، لیلا یوسف تبار میری^۳، محمد بنی مهد کیوانی^۲

۱. گروه میکروبیولوژی، دانشگاه آزاد اسلامی واحد رشت، رشت، ایران

۲. گروه شیمی، دانشکده علوم، دانشگاه پیام نور، تهران، ایران

۳. گروه شیمی آلی، دانشکده شیمی دارویی، علوم پزشکی تهران، دانشگاه آزاد اسلامی، تهران، ایران

تاریخ دریافت: ۲۳ مرداد ۱۴۰۰ تاریخ پذیرش: ۲۹ شهریور ۱۴۰۰

چکیده

در اینجا، گرده خرما به عنوان حامل داروی آمیکاسین برای اولین بار استفاده شد. گرده خرما بارگذاری شده با آمیکاسین با استفاده از میکروسکوپ الکترونی روبشی، طیف‌سنجی فرسرخ تبدیل فوریه و آنالیز سطح مشخص شد. اندازه منافذ گرده خرما ۸۰-۲۰۰ نانومتر به دست آمد که برای جذب دارو مطلوب بود. اثرات pH و دما بر روی بارگذاری آمیکاسین در گرده خرما مورد مطالعه قرار گرفت. مطالعه سینتیک رهایش دارو در بافر فسفات pH=۷,۴ و در دمای ۳۷ درجه سانتیگراد نشان داد که بهترین مدل سینتیکی معادله هیگوجی است. فعالیت ضد باکتریایی گرده خرما بارگذاری شده با آمیکاسین بر روی باکتری های استافیلوکوکوس اورئوس و اشریشیا کلی با روش انتشار آگار-چاهک بررسی شد. حداقل غلظت بازدارنده و حداقل غلظت ضد باکتری برای آمیکاسین نیز با استفاده از روش رقت برآورد انجام شد. شباهت نتایج بین حداقل غلظت بازدارنده و حداقل غلظت ضد باکتری قابل توجه است. با این حال، کاهش شدید در حداقل غلظت ضد باکتری پس از بارگذاری آمیکاسین روی گرده خرما مشاهده شد. علاوه بر این، آمیکاسین-گرده خرما برای بهبود اثربخشی آمیکاسین در برابر اشکال خطرناک باکتری های مقاوم به آنتی بیوتیک استفاده شد. به طور کلی، آمیکاسین-گرده خرما، یک روش مطلوب جهت مدیریت عفونت های باکتریایی گرم مثبت و گرم منفی را فراهم می کند و ممکن است در آزمایش های in-vivo بیشتر مورد ارزیابی قرار گیرد.

واژه‌های کلیدی

گرده خرما؛ عفونت‌های باکتریایی؛ مطالعات سینتیکی.